Driven piles installed in soft soils subjected to vertical and lateral soil movement.

Jakub G. Kania
cp test a/s, Vejle, Denmark
Kenny Kataoka Sørensen
Department of Engineering - Aarhus University, Aarhus, Denmark
Bengt H. Fellenius
Consulting Engineer, Sidney, BC, Canada

ABSTRACT
This paper presents the behavior of 406 mm diameter, 12 m long, instrumented, driven steel piles at a construction site in Esbjerg, Denmark. One pile was bitumen coated. The piles were driven through a 1.5 m thick layer of reclaimed sand underlain by naturally deposited soils consisting of a 2.0 m thick layer of sand, a 3.6 m thick layer of soft soil above a thick sand layer. The instrumentation comprised distributed fiber optic cables. Due to its spatial resolution (2.6 mm), very detailed strain profiles were obtained. The distribution of strain in the piles was induced by, first, the pile installation, building up a residual force in the piles and, then, additional force, drag force, due to negative skin friction developing after placing a 3 m thick fill around the piles. Due to construction activities an unplanned one-sided loading occurred inducing considerable bending moment and shear force in the test piles.

RÉSUMÉ
Cet article présente le comportement de pieux d'acier instrumentés et entraînés de 406 mm de diamètre et 12 m de longueur sur un chantier de construction à Esbjerg, au Danemark. Un des pieux était recouvert de bitume. Les pieux ont été enforcés à travers une couche de 1.5 m d'épaisseur de sable récupéré reposant sur des sols naturellement déposés consistant en une couche de sable de 2.0 m d'épaisseur, une couche de 3.6 m d'épaisseur de sol mou au-dessus d'une couche de sable épaisse. L'instrumentation comprenait des câbles à fibres optiques distribués sur la longueur. En raison de sa résolution spatiale (2.6 mm), des profils de déformation très détaillés ont été obtenus. La répartition de la tension dans les pieux a été induite par, tout d'abord, l'installation des pieux, en créant une force résiduelle dans les pieux et, ensuite, une force supplémentaire, une force de traînée, due au frottement cutané négatif se développant après avoir placé un remblai de 3 m d'épaisseur autour des pieux. En raison des activités de construction, un chargement unilatéral imprévu s'est produit induisant un moment de flexion et une force de cisaillement considérables dans les pieux d'essai.

1 INTRODUCTION

Understanding a soil-pile interaction is essential in a piled-foundation design. Conventionally, piles have been instrumented with telltales or strain gages in order to obtain strain distribution analysis of load distribution and to monitor the axial short- and long-term pile behavior. More recently, piles were instrumented with distributed fiber optic sensing (DFOS) systems based on Brillouin scattering (Kechavarzi et al. 2019).

This paper presents a description of instrumentation and results of tests on two instrumented steel piles driven at a construction site in Esbjerg, Denmark. One pile was bitumen coated and one was uncoated. Both were instrumented with DFOS cables using a Luna ODiSI-B interrogation unit based on Rayleigh backscattering with a 2.6 mm spatial resolution.

2 MATERIALS AND METHODS

2.1 Soil profile

The test site was located in Esbjerg, Denmark. The natural deposits at the site consisted of 2.0 m thick layer of uniform, fine to coarse sand underlain by a 3.6 m thick layer of soft, organic soil above a thick sand layer. A 1.5 m layer of reclaimed uniform fine to coarse sand was placed on top of the original sand layer. The soft soil layer is found to be of postglacial marine, organic and consisting of gyttja and peat. The bottom layer is a postglacial marine, dense, uniform, medium sand.

The soil profile, distribution of water content in the soft soil layer, and Atterberg limits are presented in Figure 1.The water content of the soft soil layer ranged from about 77 % to about 273 % with an average of 158 %. The plastic

limit, w_p, ranged from 63 % to 383 % and the liquid limit, w_l, ranged from 145 % to 499 %. An average measured unit density of the soft soil layer was about 1,200 kg/m^3.

The grain size distribution, presented in Figure 2, shows the dominant particle size, on average, to be 69 % silt size, 11 % clay size, and 20 % sand size. The organic content in the soft soil layer ranged from 12.9 to 91.4 % with an average of 56 %.

The results of two CPTU soundings pushed on February 17-20, 2017 are presented in Figure 3.The CPTU 1 and CPTU 2 sounding was pushed about 55 and 70 m from the test piles, respectively. As indicated in the enlarged portion of the qc-diagram, both results showed the existence of the soft soil layer between about 3.0 to 4.5 m depth.

Undrained shear strength of 16 kPa of the soft soil layer was determined based on the CPTU soundings applying a cone factor, Nk, of 15

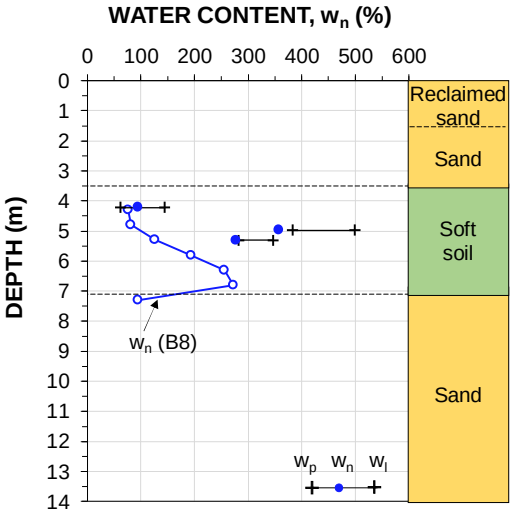

Figure 1. Soil profile, atterberg limits (soil samples collected in connection to the installation of in-situ monitoring equipment for the test setup on January 16-18, 2018) and distribution of water content (soil boring B8 performed on October 15, 2008)

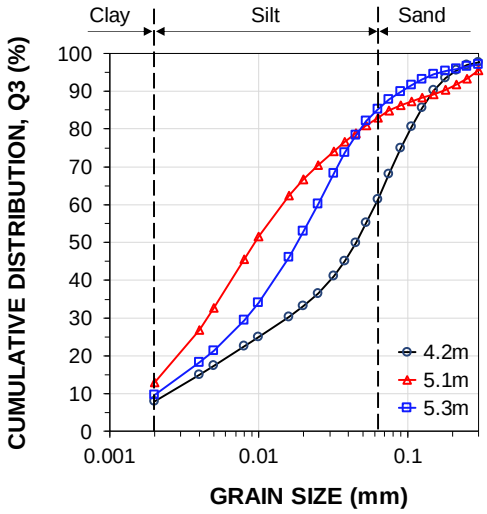

Figure 2. Grain size distribution by laser diffraction performed on soil samples collected in connection to the installation of in-situ monitoring equipment (data from Savery 2019).

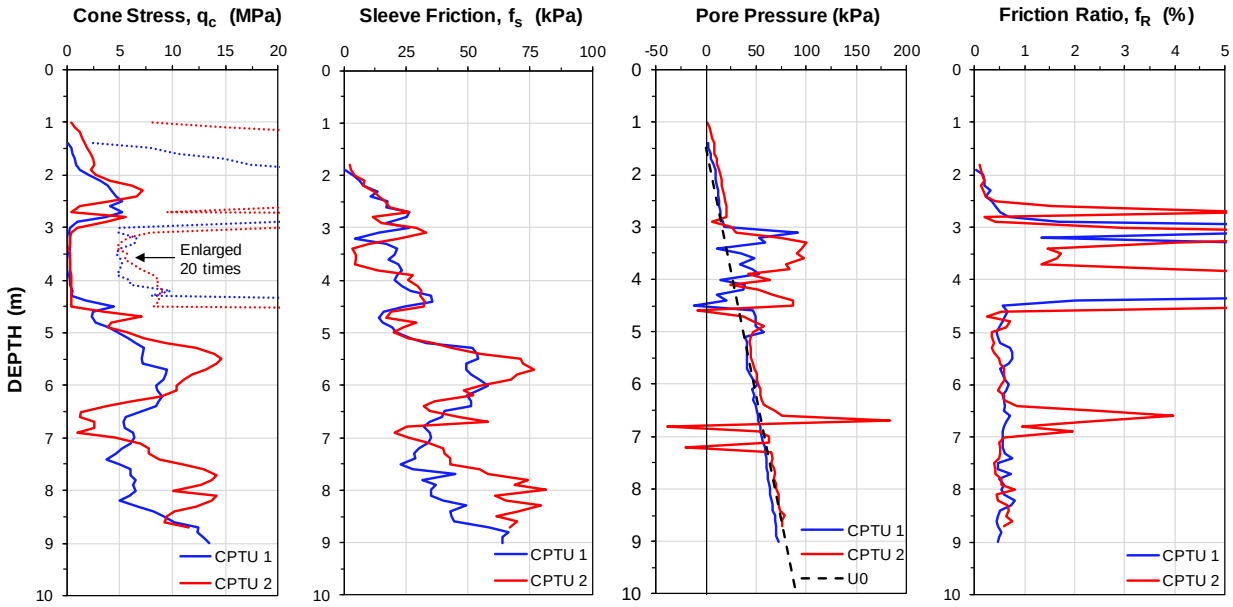

Figure 3. CPTU diagrams (CPTU 1 and CPTU 2 from soundings pushed about 55 m and 70 m from the test piles on February 17-20, 2017).

Four oedometer tests from 4.1, 4.3, 5.1, and 5.33 m depth have been carried out to determine the compressibility characteristics of the soft soil layer. From the tests Janbu modulus number, m, was found to be about 6, corresponding to a compression ratio, CR, of 0.44. The recompression modulus number, m_r, was about 48, corresponding to a recompression ratio, RR, of 0.056. The coefficient of consolidation, c_v, was about 2.9 m^2/year. The soft soil layer was normally consolidated.

2.2 Test setup and instrumentation

The test setup consisted of four instrumented test piles and a ground monitoring system (Figure 4). The test piles were two instrumented 406 mm diameter (8 mm wall thickness) steel piles (STP1 and STP2) and two instrumented 350 mm square precast concrete piles (CTP1 and CTP2). The piles were driven with a 90 kN Junttan HHK9A hammer from a working platform (elevation +1.5 m above mean sea level) to the approximate depth of 12 m. Piles STP1 and CTP1 were without bitumen coating and piles STP2 and CTP2 were coated with a 1 mm thick layer of 80/100 penetration bitumen to 8 m depth. The ground monitoring system consisted of several vibrating wire piezometers, settlement stations, and one standpipe piezometer, which all were installed from the working platform. The fill was placed up to +4.5 m ASL over approximately 125 x 150 m area around the test piles.

The pore water pressures were measured using low air-entry vibrating wire piezometers installed at 5.0, 6.5, 7.7, and 12.2 m depth using the fully grouted installation method. The grout consisted of water, cement, and bentonite with the 8:1:1 ratio by weight (water:cement:bentonite). In addition, one open standpipe piezometer was installed with the intake zone at 12.5 m depth.

The settlement at different depths was measured by magnetic extensometers (6 leaf spider magnets) installed at 1.2, 4.4, 6.1, 7.6, 8.7, and 13.4 m (datum magnet). The settlement of the surface was monitored by two settlement plates installed at 0.5 m depth.

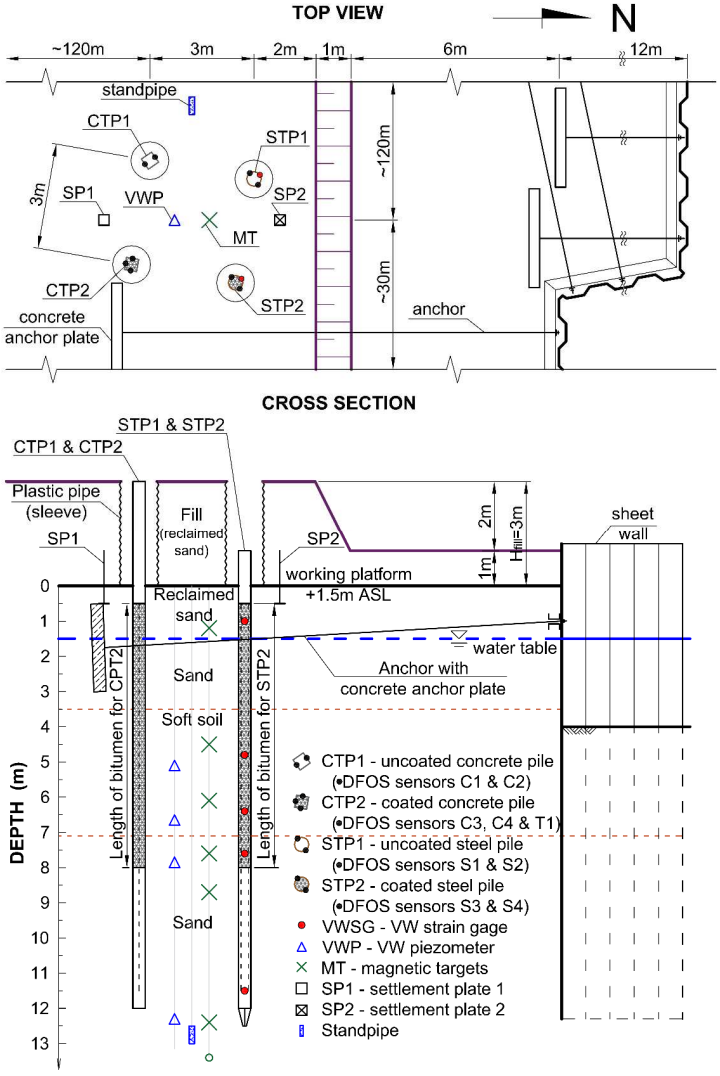

Figure 4. Soil profile and the test setup.

Figure 5 shows the instrumentation of the steel piles. A pair of opposite mounted strain DFOS cables (BRUsens V9) was used. Two Ø 12 mm steel rebars were welded (one side intermittent fillet weld with weld length of 50 mm and pitch of 150 mm) along the test piles as a guide and protection for the DFOS cables. After placing the cables along the additional rebars, the DFOS cables were pre-strained to about 1,000 με. The cables were glued using Araldite 2012 epoxy afterwards. Additionally, one line of vibrating wire strain gages (VW) was installed at five different depths: 1.0, 4.8, 6.4, 7.6, and 11.5 m respectively. The VWs were protected by an angle iron. Both steel test piles were supplied with pointed pile shoe.

Due to malfunctioning of one of the strain DFOS cables installed on the precast concrete pile, the instrumentation and the results obtained from the other strain DFOS cables will not be presented in this paper.

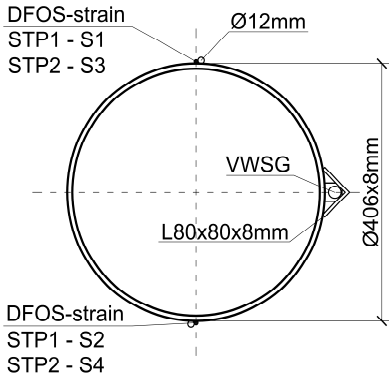

Figure 5. Cross-section of the instrumented steel test pile.

2.3 Test schedule

The planned test schedule consisted of two phases: Phase 1 to investigate the effect of the pile installation and Phase 2 to monitor the build up of drag force due to negative skin friction. The piles (steel and precast concrete) were driven on December 21, 2017 (Day 0) and the installation process took about 4 hours. The piles were installed with a 1 m stick-up above the ground surface (Depth 0). Then, on between May 1 and 3, 2018 (Days 131 through 133) placing of a 3 m thick fill around the test piles took place. Placing of the fill was completed in two 1.5 m stages. Monitoring of Phase 2 continued from May 3, 2018 through December 13, 2019 (Days 133 through 722).

The ground monitoring system was installed between January 16-18, 2018 (Days 26 through 28). The settlement and the pore water pressure data are referenced to the "zero" reading at Day 28. The strain measurements are referenced to the before-driving state, unless stated differently.

The first set of measurements was taken immediately after all four test piles had been driven, thereafter, seven sets of Phase 1 measurements were taken on Days 25, 48, 62, 78, 91, 119, and 126 until starting Phase 2 on May 3, 2018 (Day 133).

Construction activities, including installation of a sheet pile wall, anchor plates and filling the area in-between the sheet pile wall up to the final level of +4.5 m ASL, in the close proximity to the test piles continued during Phase 1 and 2 until about Day 200. As shown in Figure 6 (a), an unplanned one-sided loading occurred during Phase 1. The sheet pile wall was installed at Day 91. Further details on the construction activities around the test piles during Phase 1 are provided in Kania and Sørensen (2019). The concrete anchor plates were installed in the proximity to the test piles (about 3 m away from the bitumen coated steel pile) between Days 123-125 as presented in Figure 6 (b).

Figure 6. Test site at (a) Day 78 and (b) Day 126 (before placing the 3.0 m fill). The concrete slabs in (b) are anchor plates for the sheet pile wall seen in the background.

2.4 Data analysis

2.4.1 Temperature compensation

The strain data recorded from the DFOS cables must be thermally compensated in order to obtain mechanically induced strains. Unfortunately, the temperature DFOS cable installed on the bitumen coated precast concrete pile (see Figure 4, sensor T1 on CTP2) was damaged before the pile installation. Therefore, the temperature data with depth and time for temperature correction of the strain DFOS records were obtained using the thermistor readings from the VW gages. The point-to-point temperature correction proposed in (Luna 2014) was accordingly modified into the following:

$$\varepsilon_m^z = \varepsilon_t^z - \left(0{,}95 \cdot \frac{\Delta T^z}{k_T} \cdot k_\varepsilon + \Delta T^z \cdot \alpha_L\right) \quad (1)$$

where: ε_m^z is the mechanical strain at depth z, ε_t^z is the total (measured) strain at depth z, ΔT^z is the change in temperature at depth z, k_ε is the strain conversion factor (strain/frequency) equal to 6.67 με/GHz, k_T is the temperature conversion factor (°C/frequency) equal to 0.638 C°/GHz, α_L is the thermal expansion coefficient of steel equal to 12.2 με/C°.

2.4.2 Data interpretation

The following information was calculated from the two diametrically opposite placed DFOS cables:

$$\varepsilon_{m,a}^z = \frac{1}{2}\left(\varepsilon_{m,1}^z + \varepsilon_{m,2}^z\right) \quad (2)$$

$$\kappa^z = \frac{1}{d}\left(\varepsilon_{m,1}^z - \varepsilon_{m,2}^z\right) \quad (3)$$

$$M^z = EI\kappa^z \quad (4)$$

$$Q^z = \frac{d}{dz} EI\kappa^z \quad (5)$$

where: $\varepsilon_{m,a}^z$ is the averaged axial mechanical strain at depth z, $\varepsilon_{m,1}^z$ is the mechanical strain of cable 1, $\varepsilon_{m,2}^z$ is the mechanical strain of cable 2, κ^z is the curvature at depth z, d is the distance between two opposite strain DFOS cables, M^z is the bending moment at depth z, E is the Young's modulus of steel (210 GPa), I is the moment of inertia of the steel test piles ($1.98 \cdot 10^{-4}$ m^4), Q^z is the shear force at depth z.

Then, assuming the boundary conditions, the gradient and the lateral displacement are derived using the following equations:

$$ø^z = \int_0^z \kappa \, dz + A \quad (6)$$

$$u^z = \int_0^z ø \, dz + B \quad (7)$$

where: $ø^z$ is the gradient at depth z, u^z is the lateral displacement at depth z, A and B are the integration coefficients as determined by the boundary conditions.

3 RESULTS

3.1 Soil settlements

Figure 7 shows the soil settlement at selected days after pile driving. It can be seen from the graph, that the settlement occurred mainly due to the compression of the soft soil layer. The maximum settlement of 33 mm before placing the fill (Day 126) was recorded from the settlement gage located at 1.2 m depth. The settlement during Phase 1 is thought due to consolidation of the soft soil layer due to the placing a 1.5 m thick layer of reclaimed sand to form a working platform. Placing the additional 3 m high fill layer significantly increased the compression of the soft soil layer. The maximum settlement at Day 722 was recoded to be 381 mm as recorded at 1.2 m depth.

As shown in Figure 8, the individual settlement gages installed above 6.1 m depth are still settling albeit at a decreasing rate. The settlement after full consolidation is expected to amount to 436 mm. The settlement of the gage located at 1.2 m depth is mainly due to compression of the soft soil layer. Placing of the fill is seen to cause only small settlement of the gages located in the sand below 7.6 m depth.

Small settlements of the pile head (1-4 mm) were recorded during Phase 1 and Phase 2.

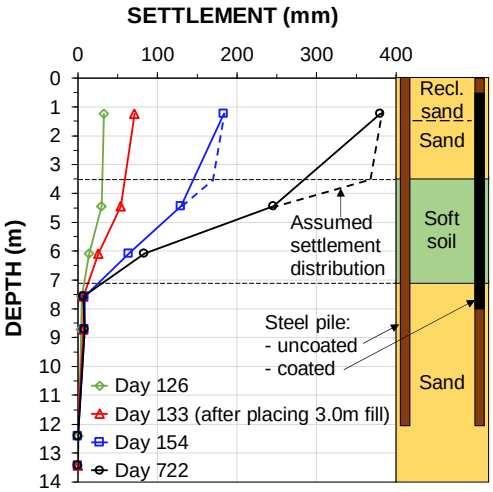

Figure 7. Soil settlement profiles at selected days after pile driving.

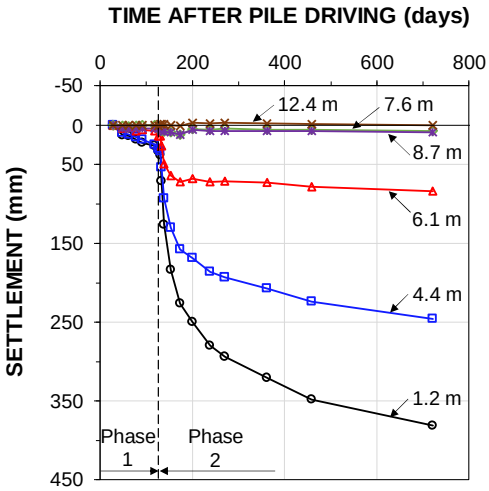

Figure 8. Settlement of individual gages with time after pile driving.

3.2 Pore water pressures

Figure 9 presents the measured pore water pressures with time. Immediately after placing the fill the piezometer located at 5.0, 6.5, and 7.7 m depth recorded an increase of 12.4, 11.5 and 8.9 kPa, respectively. The piezometer installed at 12.2 m depth (sand layer) did not record any increase of pore water pressure immediately after placing the fill. Between Day 133 and Day 141 the pore water pressure decreased by 4.9, 5.2, and 4.2 kPa from the piezometer installed at 5.0, 6.5, and 7.7 m depth, respectively. After Day 141, all the piezometers recorded an increase of pore water pressure. As can be seen from

the graph the ground water table level in the bottom sand layer was increasing after placing the fill. It is therefore likely that the reduction in the pore water pressure due to consolidation is cancelled out by the increase due to rise in the water table. The piezometer installed at 12.2 m depth was following the increase of ground water table level.

Figure 10 shows the hydrostatic and measured pore water pressure profiles at selected days after pile installation. At Day 48, the piezometer in the sand layer (12.2 m depth) showed a hydrostatic pore pressure corresponding to a ground water level at 3 m depth (1.5 m below mean sea level), while the water level measured from the ground surface corresponded to 1 m depth (0.5 m above mean sea level). The other piezometers confirmed the non-hydrostatic pore water pressure distribution. At Day 533, the piezometer installed at 5.0 m depth showed about 10 kPa excess pore water pressure, while the piezometers located at 6.5, 7.7, and 12.2 m depth showed hydrostatic distribution.

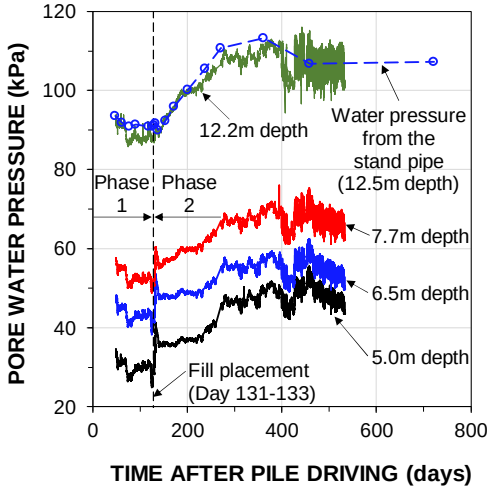

Figure 9. Pore water pressure recorded from individual piezometers located at different depths and the water pressure calculated from the standpipe water level records.

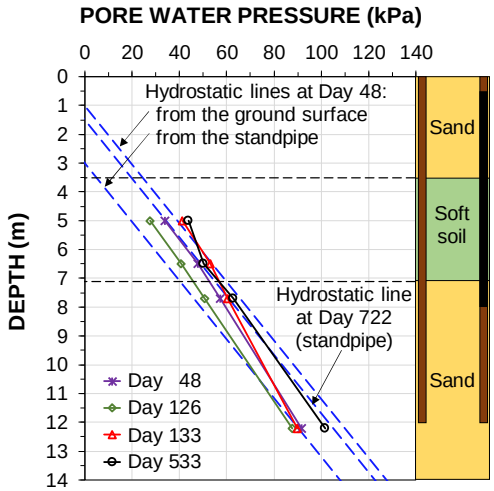

Figure 10. Pore water pressure profiles at selected days after pile driving.

3.3 Strain distributions

Figure 11 shows the strain distribution obtained from the individual strain DFOS cables along (a) the uncoated and (b) bitumen coated steel pile at selected days after pile driving. Negative values denote compression. To smoothen the strain DFOS data, a moving average over 100 readings was calculated giving a virtual gage length of 0.26 m. The strain records obtained immediately after driving (Day 0) from the uncoated (STP1) and bitumen coated (STP2) steel pile indicate bending of the piles. The observed increase in strain between Day 0 and Day 126 (before placing the fill around the test piles) i.e., S1 and S3—increase in tension and S2 and S4—increase in compression, could be attributed to the aforementioned unplanned one-sided loading occurring before Day 126 and causing bending of the piles. The maximum compression and tension values were recorded around the boundary between the soft soil and the bottom sand layer.

Due to the bending, the readings obtained from the single line of VW gages were not analysed and are not presented in this paper.

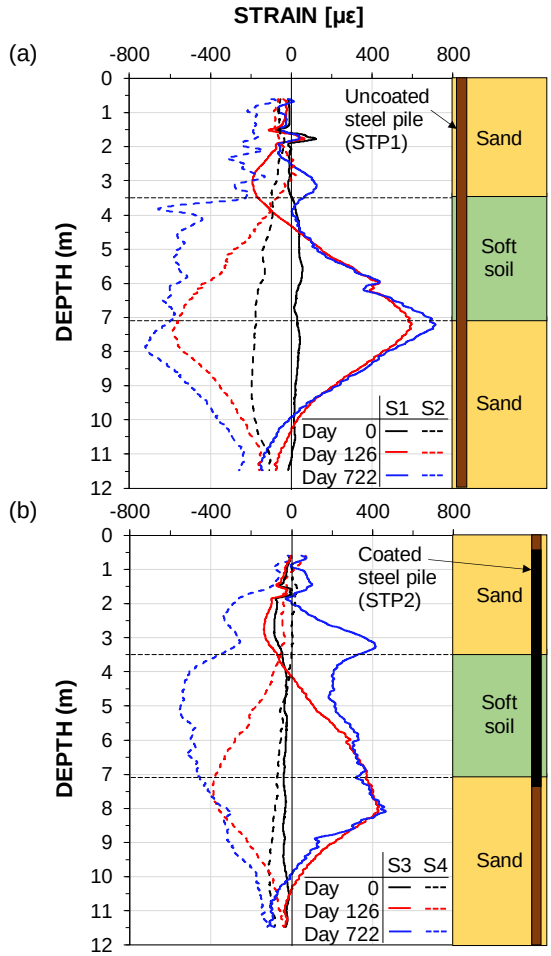

Figure 11. Strain profiles in (a) the uncoated steel pile (sensor S1 and S2) and (b) coated steel pile (sensor S3 and S4). The plots show measured data immediately after driving (Day 0), before placing the fill (Day 126), and 589 days after placing the fill (Day 722).

4 ANALYSIS

4.1 Deformation of the test piles

In order to investigate the deformation of the test piles, it was assumed that the piles worked as cantilever beam fixed at the pile toe after driving. The reference readings were those recorded immediately after driving. This allowed to determine the integration coefficients (cf. Eqs. 6 and 7). Figure 12 shows the curvature (a) and (d), gradient (b) and (e), and the lateral displacement (c) and (f) of the uncoated and bitumen coated steel pile, respectively. It can be seen from the graphs that both piles experienced similar deformation before placing the fill (Day 126). Afterwards (Day 722), the curvature, gradient, and lateral displacement of the uncoated steel pile (STP1) increased above 10.5 m depth. In contrast, the lateral deformation of the bitumen coated steel pile (STP2) was unchanged below 7.5 m depth.

4.2 Influence of the pile deformation on the distribution of internal forces.

Figure 13 shows the distribution of axial force (a) and (d), the bending moment (b) and (e), and the shear force (c) and (f) along the uncoated (STP1) and bitumen coated (STP2) steel pile respectively. These features were determined directly from the strain data with reference readings before pile driving. Positive values of axial force denote compression. In order to obtain an appropriate shear force distribution, the bending moment was smoothened (using a moving average) before differentiation. Even though, the shear force diagram above 4.5 m depth along the STP1 was scattered (Figure 13 (c)). Smoothening the data should be used with caution, since it can easily alter or disguise the meaningful data points.

It can be seen from the graphs in Figure 13 that the development of internal forces immediately after driving (Day 0) and during the Phase 1 (Day 126) was similar in both test piles. Placing of the fill (Day 722) changed the bending moment and the shear force distribution, which significantly affected the axial force profiles. The bending moment increased along the uncoated and bitumen coated steel test pile. However, interestingly, it reached a constant value in the soft soil layer along the bitumen coated steel pile (Figure 13 (e)). The constant bending moment resulted in a neutralization of the shearing force in the soft soil layer. The presence of shear forces, especially at the boundaries between sand and the soft soil layer (at 3.5 and 7-8 m depth), generated tensile strain within the shear plane and affected the interpretation of axial force distribution.

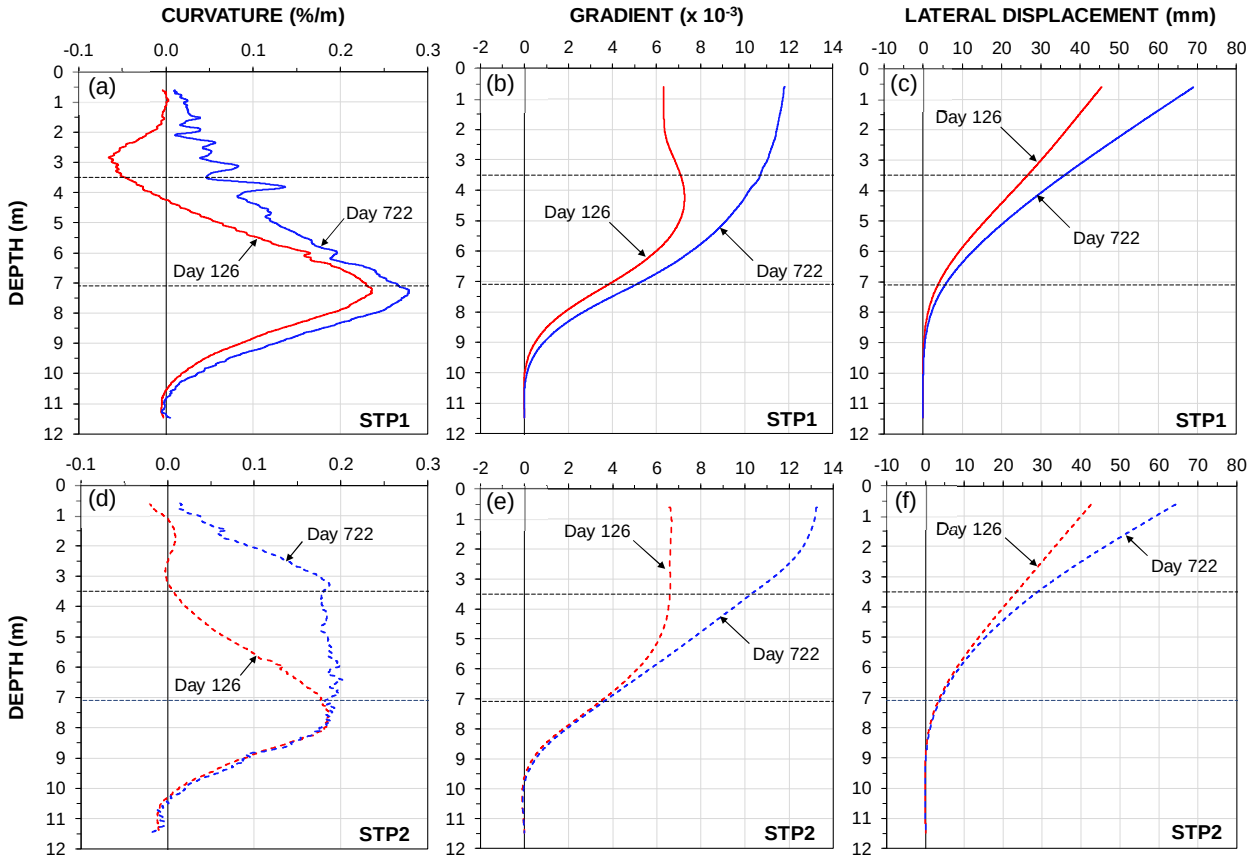

Figure 12. Curvature ((a) and (d)), gradient ((b) and (e)) and lateral displacement ((c) and (f)) of the uncoated (STP1) and bitumen coated (STP2) steel test pile recorded at Day 126 (before placing the fill) and Day 722 (589 days after the end of placing the fill). Data for STP1 at Day 126 from Kania et al. 2020.

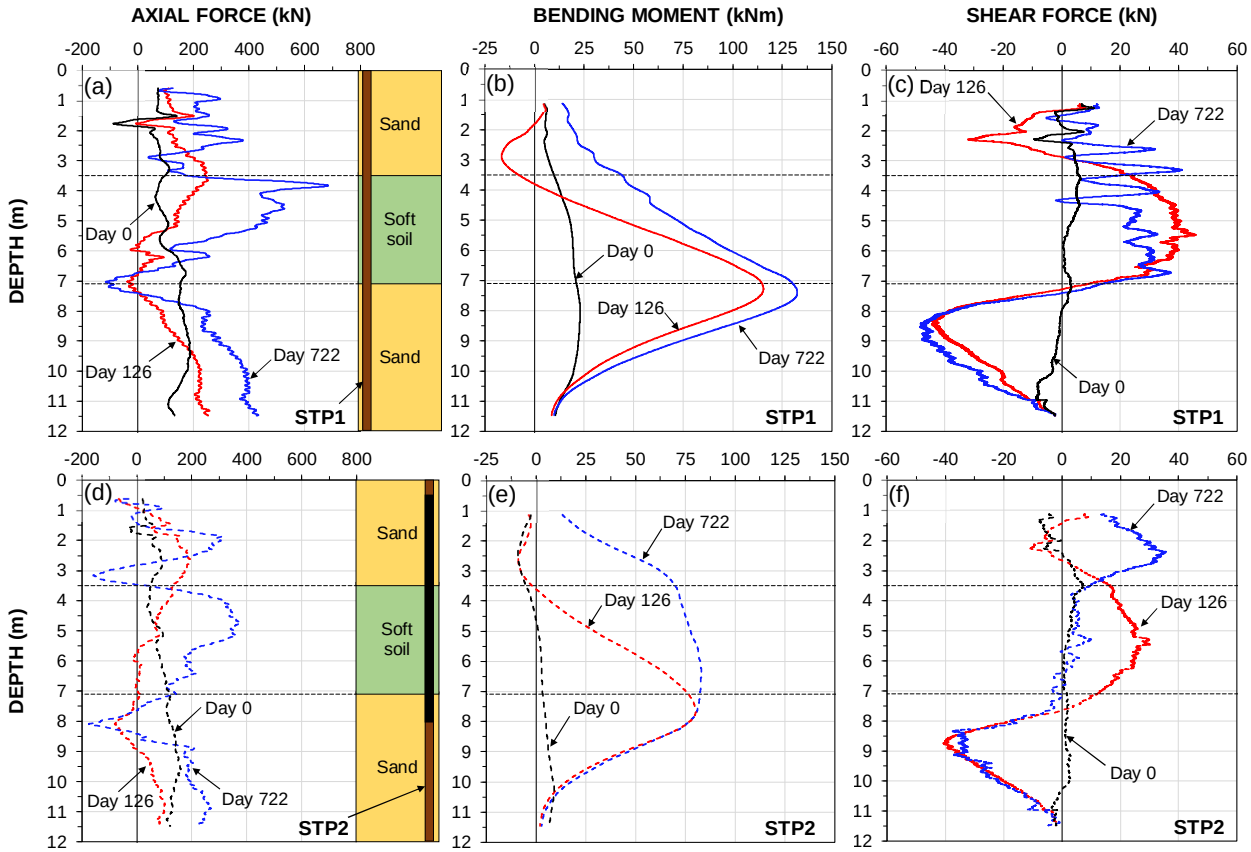

Figure 13. Axial force ((a) and (d)), bending moment ((b) and (e)) and shear force ((c) and (f)) along the uncoated (STP1) and bitumen coated (STP2) steel test pile recorded at Day 0 (immediately after driving), Day 126 (before placing the fill) and Day 722 (589 days after the end of placing the fill).

5 CONCLUSIONS

Driven piles instrumented with DFOS cables can provide detailed information about the strain distribution. At least a pair of opposite mounted cables should be installed to determine the influence of lateral and vertical soil movement.

To obtain mechanically induced strains, recorded strain data from DFOS cables must be thermally corrected.

Axial strain, curvature and bending moment are directly obtained from the strain measurements. Therefore, they are more reliable than the gradient and lateral displacement distribution, which requires assumptions regarding boundary conditions.

Although shear force distribution can be calculated by differentiation of a bending moment, the bending moment distribution should be smoothened to obtain an appropriate shear force profile. However, smoothening must be applied with caution because it can disguise sudden data changes.

The distribution of axial force was induced by the pile installation, building up a residual force in the piles, and placing of the fill. However, it was disturbed by the bending moment and shear force in the test piles caused by lateral soil movement. The presence of shear forces generated tensile strain at the location of shear planes and influenced the interpretation of axial force distribution.

6 ACKNOWLEDGMENTS

The authors would like to thank cp test a/s, Per Aarsleff A/S, Centrum Pæle A/S, DMT Gründungstechnik GmbH and Innovation Fund Denmark for providing funding for this study and Per Aarsleff A/S for providing data and for installing the instrumented test piles.

7 REFERENCES

Kania, J.G. and Sørensen, K.K. 2019. A case study of soil-pile interaction in soft soils. *XVII European Conference on Soil Mechanics and Geotechnical Engineering*, Reykjavik, Iceland.

Kania, J.G., Sørensen, K.K. and Fellenius, B.H. 2020. Application of distributed fibre optic cables in piles. *Geotechnical Engineering Journal of the SEAGS and AGSSEA*, 51(1), 94-102.

Kechavarzi, C., Soga, K.B., Battista, N.D., Pelecanos, L., Elshafie, M.Z.E.B. and Mair, R.J. 2016. *Distributed fibre optic strain sensing for monitoring civil infrastructure - a practical guide,* ICE Publishing, London, UK, 264 p.

Luna Inc. 2014. Distributed Fiber Optic Sensing: Temperature Compensation of Strain Measurement. Engineering note EN-FY1402, Roanoke, Virginia, United States, 7 p.